AIAA JOURNAL
Vol. 30, No. 2, February 1992

Numerical Study of Vibration Localization in Disordered Cyclic Structures

Phillip J. Cornwell* and Oddvar O. Bendiksen†
Princeton University, Princeton, New Jersey 08544

A study of mode localization in disordered cyclic structures that have multi-degree-of-freedom substructures in presented. Particular emphasis is placed on the transition of the natural modes from being extended throughout the structure to being localized on a single substructure. A localization length scale is proposed as a measure of the spatial extent of a mode for the purpose of discussing the results of numerical experiments and comparing the localization of different modes. Different modes in the same mode group were found to have significantly different degrees of localization, and similar modes in different mode groups were found to be related to each other via a scaling parameter. Results also indicate that the particular set of random disorder introduced into the finite structure can have a significant effect on the degree of localization.

Nomenclature

A	= cross-sectional area of axial member
EI	= rib flexural rigidity
k_i	= effective stiffness of axial member
$[K]$	= global stiffness matrix
l	= total length of rib
l_a	= length of axial member
L^*	= normalized localization length scale
$[M]$	= global mass matrix
m	= rib mass per unit length
N	= total number of ribs
N^*	= localization length scale
n	= circumferential wave number
p	= number of degrees-of-freedom per substructure
Q_i	= generalized force
q_i	= generalized coordinate
$\tilde{q}_i$	= amplitude of q_i
r	= imperfection strength
T	= total kinetic energy
U	= total potential energy
V_i	= potential energy due to the axial member between rib i and $i+1$
$v(x,t)$	= displacement of in-plane motion
$w(x,t)$	= displacement of out-of-plane motion
$\bar{x}$	$= x/l$
γ	= localization factor
θ	= half-angle between ribs
λ	$= (\omega/\omega_o)^2$ = eigenvalue
$\Delta\lambda$	= normalized eigenvalue band
σ	$= 2\pi n/N$
ω	= natural frequency
ω_o	$= \sqrt{EI/ml^4}$ = reference frequency
$\tilde{\omega}$	$= \omega/\omega_o$ = nondimensional frequency
$\phi_n(x)$	= mode shape function

Received Sept. 19, 1989; revision received June 5, 1990; accepted for publication June 5, 1990. Copyright © 1990 by the American Institute of Aeronautics and Astronautics, Inc. All rights reserved.

*Graduate Student; currently Assistant Professor, Mechanical Engineering Department, Rose-Hulman Institute of Technology, Terre Haute, IN 47803.

†Assistant Professor; currently Associate Professor, Mechanical, Aerospace, and Nuclear Engineering Department, University of California, Los Angeles, CA 90024. Member AIAA.

Introduction

PERIODIC structures that are characterized by a number of weakly coupled substructures have been shown to be sensitive to certain types of disorder.[1-7] This disorder could arise form such factors as manufacturing or assembly errors. When structural imperfections are introduced into the structure, natural modes that were originally extended throughout the structure can become confined or localized to a small region of the structure. In applications where accurate shape control is required, such as in large astronomical telescope reflectors and communication antennas, the presence of localized modes would be undesirable. It is therefore important to consider structural imperfections when designing control systems for shape or directional control of such structures.

Extensive numerical calculations have been done showing the progressive evolution of a mode from being extended throughout the structure to being localized to a relatively small number of substructures.[6] In the case where the natural modes of the imperfect structure are only slight perturbations of the modes in the perfect structure, standard perturbation techniques can be used to describe the natural modes. Similarly, when a mode is extremely localized and its spatial extent is limited to only a few substructures, the modified perturbation method (MPM) introduced by Pierre[7] does a very good job of predicting the shape and frequency of the mode. The case where the mode is between these two extremes is the one that is difficult to characterize. The mode may be localized in the sense that it is not extended throughout the structure, but it still may have a significant magnitude over much of the structure. While investigating the phenomenon of mode localization in finite periodic structures, the question that arises is what constitutes a "localized" mode? For localization in the setting of solid-state physics, several "localization length scales" have been proposed[8-9] to measure the spatial extent of a mode. These length scales are useful in discussing the results of numerical experiments and in understanding the trends associated with localization, but in general cannot be calculated a priori. The localization factor γ that describes the exponential decay of the amplitude of a mode is one characterization of mode localization that can in some cases be calculated analytically. Thus far, the only analytical results obtained in structural dynamics are for systems that can be modeled with a 2×2 transfer matrix, or equivalently a tridiagonal stiffness matrix.[11-12] In this paper, the localization phenomenon for a structure with multidegree-of-freedom (MDOF) substructures will be investigated via numerical experiments.

This paper is primarily a continuation of the work described in Ref. 6 concerning the localization of natural modes in cyclic periodic structures such as large space reflectors. In Ref. 6 structures of this type were found to be susceptible to localiza-

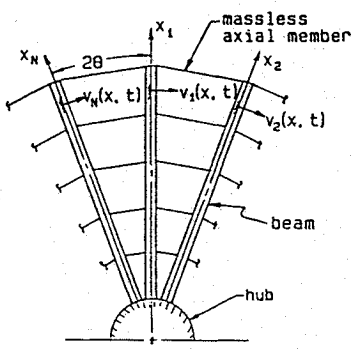

Fig. 1a Structural model for axially symmetric structure such as a radial rib reflector/antenna.

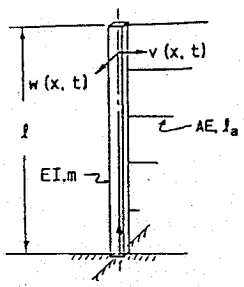

Fig. 1b Typical substructure, consisting of rib beam and sectional wires (axial members).

tion. The localization was found to become progressively more severe with increasing mode group. This result has also been obtained by Pierre.[7] The evolution of the frequencies as a function of the imperfection strength was also examined in Ref. 6. As the imperfection strength is increased from zero, some of the natural frequencies were found to come very close together and then to veer away from each other. A strong interaction was observed between the two veering modes, as indicated by the exchange in the localization peaks.

In the present paper, localization in a generic class of reflectors is studied with the intent of better understanding the phenomenon in finite structures with MDOF substructures. A normalized localization length scale L^* is introduced as a characterization of the degree of localization in order to study the transition from extended states to localized states and to provide a convenient way of comparing the degree of localization of different modes. A definite relationship is found to exist between the mode groups and how they localize. The normalized eigenvalue band presented in Ref. 6 as a measure of the effective coupling between substructures is found to serve as a scaling parameter and can be used to relate the localization behavior and the frequency evolution of the various mode groups for the model studied. The effective coupling between substructures is an indicator of the relative susceptibility of a mode group to localization.[6,7] The influence on the localization of the particular set of random imperfections introduced into the structure is also examined for the first time.

Structural Models

For the class of axially symmetric structures considered in this study (Fig. 1), the basic substructure consists of one of the N radial beams (ribs) with the associated connecting axial member. The structural model used for most of the analysis is a Rayleigh-Ritz model based on the first five cantilever-beam bending modes for each radial rib. The coupling between substructures is provided by a single massless axial member (spring) that could model anything from a wire mesh to a web membrane. In Ref. 6, it was shown that using multiple connecting wires does not change the shape of the natural modes significantly, provided the effective coupling remains the same. The hub of the structure is considered to be fixed.

For small-amplitude vibrations, in-plane and out-of-plane vibrations decouple and can therefore be considered separately. The vibration displacement of the ith beam in the plane of the structure is denoted by $v_i(x,t)$, and the corresponding out-of-plane displacement is denoted by $w_i(x,t)$ (Fig. 1b). In this paper, the structure will be assumed to be flat so the only difference between the equations of motion for the in-plane and the out-of-plane motion is the physical interpretation of the coupling k_c.

Rayleigh-Ritz Model

For the Rayleigh-Ritz model, the in-plane displacement of a rib can be written as

$$v_i(x,t) = \sum_{n=1}^{p} q_n(t)\,\phi_n(x) = \{q\}_i^T\{\phi\} \tag{1}$$

where the mode shapes $\phi_n(x)$ is the nth natural mode of a cantilever beam and are given in the Appendix. In this study, the first five cantilevered beam modes were used, that is $p = 5$. The equations of motion are determined using Lagrange's equations:

$$\frac{d}{dt}\left(\frac{\partial T}{\partial \dot{q}_i}\right) - \frac{\partial T}{\partial q_i} + \frac{\partial U}{\partial q_i} = 0 \tag{2}$$

where T is the total kinetic energy

$$T = \sum_{i=1}^{N} T_i = \sum_{i=1}^{N} \frac{1}{2}\{\dot{q}\}_i^T[M]_i\{\dot{q}\}_i \tag{3}$$

$$[M]_i = \int_0^l m_i\{\phi\}\{\phi\}^T dx \tag{4}$$

and U is the total potential energy that is the sum of the stain energy due to the bending of the beams and the strain energy in the axial members between the ribs:

$$U = \sum_{i=1}^{N} \frac{1}{2}\{q\}_i^T[K]_i\{q\}_i + \sum_{i=1}^{N} V_i \tag{5}$$

where

$$[K]_i = \int_0^l EI_i\{\phi''\}\{\phi''\}^T dx \tag{6}$$

$$V_i = \tfrac{1}{2}k_i[v_i(h,t) - v_{i+1}(h,t)]^2 \tag{7}$$

$$= \tfrac{1}{2}k_i(\{q\}_i^T\{\phi(h)\} - \{q\}_{+1}^T\{\phi(h)\})^2 \tag{8}$$

Here, k_i is the effective stiffness of the spring between beams i and $i + 1$, and h is the location of the axial member along the beams. It has been shown[4,12] that variations in the coupling k_i have a very small effect on the dynamics in comparison to variations in the flexural rigidity EI, and will therefore be considered a constant, $k_i = k_c = \text{const}$. A random variation is introduced into the flexural rigidity such that

$$EI_i = EI_0(1 + P_i) \tag{9}$$

where P_i is a random variable having a uniform distribution between r and $-r$, where r is defined to be the imperfection strength. Substituting Eqs. (3–9) into Eq. (2) results in a system of $pN \times pN$ equations:

$$[M]\{\ddot{q}\} + [K]\{q\} = 0 \tag{10}$$

where

$$\{q\}^T = \{\{q\}_1^T|\{q\}_2^T|\cdots|\{q\}_N^T\} \tag{11}$$

For small-amplitude free vibration, one can assume simple harmonic motion $\{q\} = \{\bar{q}\}e^{i\omega t}$, which when substituted into Eq. (10), leads to well-known structural eigenvalue problem:

$$[\bar{K}]\{\bar{q}\} = \bar{\omega}^2[\bar{M}]\{\bar{q}\} \tag{12}$$

where $\bar{\omega}^2 = (\omega/\omega_0)^2$; $\omega_0^2 = (EI/ml^4)_{\text{ref}}$ and $[\bar{K}]$ and $[\bar{M}]$ are the nondimensional stiffness and mass matrix, respectively. Because the normalized cantilevered beam modes were used as the shape functions, we find

$$[\bar{M}] = [I] \tag{13}$$

$$[\bar{K}] = \begin{bmatrix} \ddots & \ddots & [0] & \cdots & [0] & [K_1] \\ \ddots & \ddots & \ddots & [0] & \vdots & [0] \\ [0] & [K_1] & [K_1]+[\delta K_{ii}] & [K_1] & [0] & \vdots \\ \vdots & [0] & \ddots & \ddots & \ddots & [0] \\ [0] & \vdots & [0] & \ddots & \ddots & \ddots \\ [K_1] & [0] & \cdots & [0] & \ddots & \ddots \end{bmatrix} \tag{14}$$

where

$$[K_0] = [\text{diag}(\lambda_{j0})] + \bar{k}_c\{\phi\}\{\phi\}^T|_h \tag{15}$$

$$[K_1] = -\bar{k}_c\{\phi\}\{\phi\}^T|_h \tag{16}$$

$$[\delta k_{ii}] = P_i\,[\text{diag}\,(\lambda_{i0})] \tag{17}$$

and the normalized coupling $\bar{k}_c = k_c/(EI/ml^3)$, and λ_{j0} is the jth normalized natural frequency of a cantilevered beam as shown in the Appendix. Solving Eq. (12) numerically results in pN eigenvalues $\bar{\omega}_n^2$ and eigenvectors $\{\Psi_n\}$. For the model studied, the eigenvalues are found to be clustered in groups. In the first mode group, the ribs are primarily in first bending. Similarly, the second mode group is primarily second bending, and so forth.

Normalized Eigenvalue Band

Structures with high modal densities, that is, narrow frequency bands, have been shown to be susceptible to mode localization. The normalized eigenvalue band

$$\Delta\lambda_j = \left.\frac{\bar{\omega}_{\max}^2 - \bar{\omega}_{\min}^2}{\bar{\omega}_{\min}^2}\right|_{j=\text{fixed}} \tag{18}$$

has been proposed as measure of the effective coupling strength for a particular mode group: $j = 1$ to p. It was shown in Ref. 13 that for a single degree-of-freedom (SDOF) per substructure model Eq. (18) is directly proportional to the coupling k_c. A value of $\Delta\lambda_j$ close to zero would indicate that the modes belonging to that group would be sensitive to imperfections and might localize. An approximate expression for the eigenvalue band $\bar{\omega}_{\max}^2 - \bar{\omega}_{\min}^2$ for a given mode group j can be calculated for the perfect structure. As seen in Eq. (14), the stiffness matrix is cyclic when the random variation P_i is equal to zero. That is, the $(n+p)$th row of the stiffness matrix is a cyclic permutation of the nth row, consisting of a circular shift right by p positions. Similarly, the $(m+p)$th column is a cyclic shift down by p positions of the mth column. Using a simple transformation;

$$\{q\} = [B]\{q\} \tag{19}$$

$$\{z\}^T = \{\{z\}_1^T|\{z\}_2^T|\ldots|\{z\}_N^T\} \tag{20}$$

where the $Np \times Np$ transformation matrix $[B]$ is

$$[B] = \begin{bmatrix} [B]_{11} & [B]_{12} & \cdots \\ [B]_{21} & [B]_{22} & \\ \vdots & & \ddots \end{bmatrix} \tag{21}$$

$$[B]_{jk} = e^{i\sigma k-1(j-1)}[I_p] \tag{22}$$

$$i = \sqrt{-1} \tag{23}$$

and $[I_p]$ is a unitary matrix of order p, the $pN \times pN$ eigenvalue problem of Eq. (12) can be reduced to a series of $N/2+1$ eigenvalue problems of order $p \times p$:

$$\lambda\{z_n\} = [Q_n]\{z_n\} \tag{24}$$

$$[Q_n] = [K_0] + 2[K_1]\cos\sigma_n \tag{25}$$

$$\sigma_n = 2\pi n/N, \qquad n = 0,1,2,\ldots, N/2 \tag{26}$$

To get an approximate analytical expression for the eigenvalues of this $p \times p$ system, we apply a perturbation-type method using the coupling $\bar{k}_c$ as the perturbation parameter. The magnitude $\bar{k}_c$ for which this expansion will be valid will be discussed later. Substituting Eqs. (15-16) into Eq. (24), we find

$$[Q_n] = [\text{diag}(\lambda_{j0})] + 2\bar{k}_c\{\phi\}\{\phi\}^T|_h(1-\cos\sigma_n) \tag{27}$$

$$= [Q_0] + [\delta Q_n]$$

If $\bar{k}_c$ is relatively small, we can use ordinary perturbation methods to determine the effect the coupling will have on the natural frequencies. If we let

$$\lambda_n^{(j)} = \lambda_{j0} + \epsilon\nu_n + \epsilon^2\mu_n \tag{28}$$

we find

$$\epsilon\nu_n = 2(1-\cos\sigma_n)\bar{k}_c\phi_j^2(h) \tag{29}$$

$$\epsilon^2\mu_n = 4\bar{k}_c^2(1-\cos\sigma_n)^2 \sum_{\substack{i=1 \\ i\neq j}}^{p} \frac{(\phi_i(h)\phi_j(h))^2}{\lambda_{j0}-\lambda_{i0}} \tag{30}$$

where the subscript j refers to the jth mode group, and n refers to the nth mode in that mode group. The lowest natural frequency for each mode group occurs when $n = 0$ and so $\lambda_{\min j} = \lambda_{j0}$. If we assume the connecting spring is located at the tip, then $\phi_i(1) = \phi_j(1) = 2$ and the maximum natural frequency for mode group j is

$$\lambda_{\max}^{(j)} = \lambda_{j0} + 16\bar{k}_c + 256\bar{k}_c^2 \sum_{\substack{i=1 \\ i\neq n}}^{p} \frac{1}{\lambda_{j0}-\lambda_{i0}} \tag{31}$$

Since the mode groups are widely separated (as seen in the Appendix), the factor $\lambda_{j0} - \lambda_{i0}$ will be vary large making the third term in Eq. (31) very small. For $j = 2$, it can be shown that for $\bar{k}_c < 3$ the second-order correction $\epsilon^2\mu < 0.10\epsilon\nu$, and gets progressively smaller for $j > 2$. The values of $\bar{k}_c$ used in this study are less than this value. A comparison between the results for the frequencies using Eq. (31) and the frequencies obtained by solving the full $p \times p$ eigenvalue problem of Eq. (24) is shown in Table 1, for a value of $k_c = 3EI/l^3$. This indicates that because frequency bands are so widely separated there is not very much interaction between mode groups. From Eqs. (28-30) we see that $\lambda_{\max_j} - \lambda_{\min_j} \approx 16\bar{k}_c$ and is independent of the mode group for $j > 2$. From Eqs. (29) clearly the frequency band is proportional to the coupling $\bar{k}_c$ and the displacement at the coupling location $\phi^2(h)$. Thus, the

Table 1 Comparison of the eigenvalue band calculated by solving the full eigenvalue problem of Eq. (24) and the approximation obtained from Eqs. (29-30) with $n = N/2$, $k_c = 3EI/l^3$, and a single axial member located between the tips of adjacent structures

Mode Group	$\lambda_{max} - \lambda_{min}$ Eq. (24)	$\epsilon\mu_n$ Eq. (29)	$\epsilon^2\mu$ Eq. (30)	$\epsilon\mu_n + \epsilon^2\mu$	%difference
1	42.5246	48	−5.692	42.308	0.509
2	51.7318	48	3.963	51.963	−0.447
3	49.0267	48	1.014	49.014	0.026
4	48.4448	48	0.438	48.438	0.0153
5	48.2720	48	0.276	48.276	−0.0083

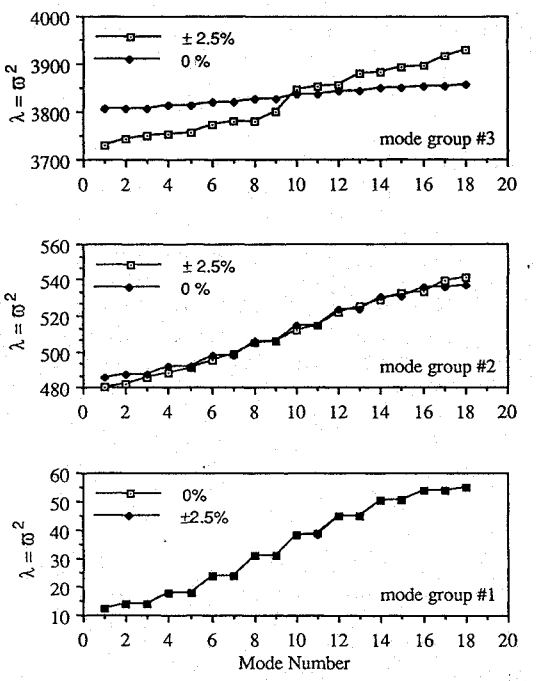

Fig. 2 Frequency bands for the first three mode groups for a structure with 18-ribs, and $k_c = 3EI/l^3$. Note the frequencies are much further apart for the higher frequency mode groups.

normalized eigenvalue band is similar to the "modal" coupling parameter R^2 introduced by Pierre[7]:

$$R_j^2 = \frac{k_c \phi^2(h)}{\lambda_{j0} M_j} \tag{32}$$

This paper will examine the case where the spring is located at the tip so as to avoid the special case of when the connecting member is located at the node of one of the beam bending modes. Clearly Eqs. (18) and (32) will capture the same trends. Since the absolute magnitude of the frequency band is virtually constant for the different mode groups, the important factor in determining the relative susceptibility to localization of the different mode groups in Eqs. (18) and (32) is the $1/\bar{\omega}^2_{min}$. This can be understood physically in terms of what happens to the natural frequencies of the ribs. The natural frequencies of the various modes of the individual ribs change by the same percentage as indicated by Eq. (9) since the frequency squared is directly proportional to the flexural rigidity, but the absolute variation is significantly different. Hence, if we consider each mode group to be modeled as SDOF oscillators with the same natural frequency as the disordered rib, then clearly the higher frequency mode groups are going to have natural frequencies for the disordered case which are much farther apart then the lower frequency mode groups. If localization is then thought of in terms of the resonant properties of the individual members, then clearly the higher mode groups will be more localized since the resonant frequencies are farther apart. To illustrate this, the frequency band of the first and the third mode groups for a structure with 18-ribs and $k_c = 3EI/l^3$ is shown in Fig. 2.

Localization Length Scales

When examining the results of computer experiments to study the localization of the eigenstates of a disordered periodic structure, some length scale or measure of the degree of localization is desirable. By defining a length scale, modes within the same mode group and in different mode groups can readily be compared. The number of substructures over which a mode has appreciable strength in comparison to the number of structures participating in the perfect structure is a good indication of that mode's degree of localization. We propose the parameter

$$N_k^* = \left(\sum_{i=1}^{N} v_i^2(l) \right)^2 / \sum_{i=1}^{N} v_i^4(l) \Big|_{k = \text{fixed}}, \qquad k = 1,2,\ldots \tag{33}$$

as a measure of the spatial extent of mode k, expressed as the number of participating substructures. The tip displacements $w_i(l)$ are used because for the structures studied the tips tended to have the maximum displacement. This quantity is virtually identical to the measure, presented in Ref. 8 for a harmonic disordered linear chain. In Ref. 8, the displacement of the atom was used in the formula.

If a mode is such that the tip displacement of each rib has the same magnitude, as would be the case in the umbrella mode or the 180 deg out-of-phase mode of the perfect structure, then N^* is equal to N, the number of substructures. If the mode is such that it is localized at one substructure, then $N^* = 1$. It should be remembered that since there are nodes in the modes of the perfect structure, some the ribs will have zero displacement and therefore do no "participate" in the mode. In order to account for the fact that N_k^* will not equal N for the perfect structure, except for the two modes mentioned above, we defined for the kth mode

$$L_K^* = N_K^* / N_{0_k}^* \Big|_{k = \text{fixed}}, \qquad k = 1,2,\ldots \tag{34}$$

where $N_{0_k}^*$ is the value of N^* for the kth mode of the perfect structure. Thus, $L_k^* = 1$ for every mode of the perfect structure. The normalized length scale L_k^* can be thought of as approximating the fraction of the number of substructures participating in the disordered structure compared with the number participating in the perfect structure. This makes it easier to compare how the spatial extent of a particular mode varies as disorder is introduced. L_k^* is also easy to calculate and is independent of the absolute magnitude of the tip displacement. The value of N_k^* can be calculated analytically if the natural mode has the form of a perfect sine wave and is equal to

$$N_k^* = (2/3)\, N \tag{35}$$

If the natural mode is a perfect exponential curve, that is the tip displacements fall off from a peak with the form $e^{-\gamma n}$, then N_k^* can be calculated to be approximately

$$N_k^* = \begin{cases} \dfrac{2}{\gamma} \tanh \dfrac{\gamma N}{2}, & \gamma < \gamma_1 \qquad \text{(36a)} \\ \dfrac{[\coth(\gamma)]^2}{\coth(2\gamma)}, & \gamma > \gamma_1 \qquad \text{(36b)} \end{cases}$$

where γ_1 is not clearly defined and depends on the number of substructures. Equation (36b) is derived for the limit $N \to \infty$ and is most accurate when $N_k^* < N/3$. Equation (36a) is a good approximation when $\gamma_1 \approx 0.2$ and $N > 10$. Figure 3 compares the value of N_k^* calculated for a perfect exponential curve

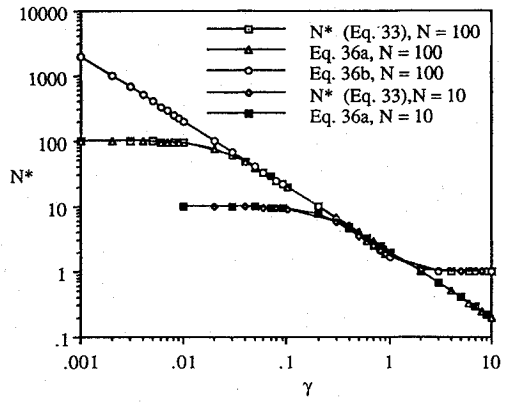

Fig. 3 Comparison of analytical expressions for calculating N^* for a mode with the form of a perfect exponential, that is the tip displacements of the ribs drop off from a maximum peak with the form of $e^{-\gamma n}$.

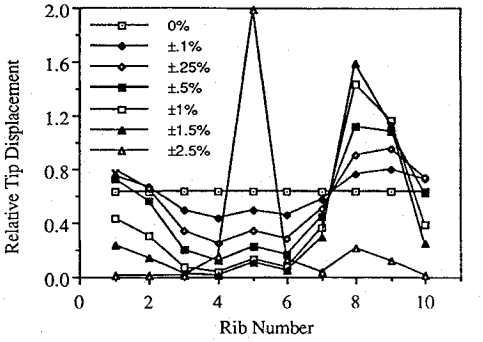

Fig. 5 Illustration of the progressive localization when the same ribs used to generate Fig. 4 are rearranged. Note the difference in the way the mode localizes and the abrupt change in the localization peak.

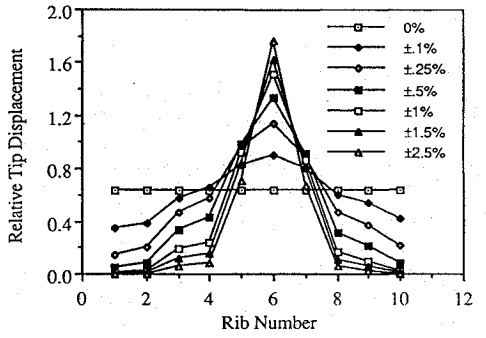

Fig. 4 Illustration of the progressive localization of the $n = 0$ mode of the third mode group ($k_c = 3EI/l^3$, $N = 10$). Notice how the mode localizes in a relatively smooth manner.

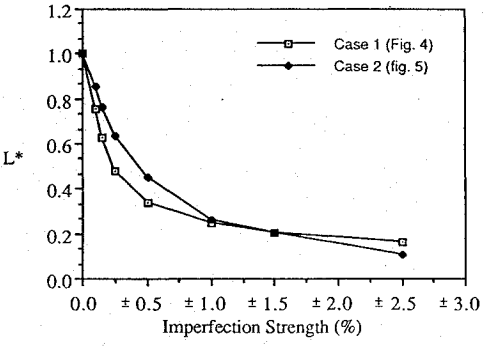

Fig. 6 Illustration of how the spatial extent of the modes shown in Figs. 4 and 5 decrease in roughly an exponential manner. L^* remains a relatively smooth function in spite of the fact that the modes undergo abrupt changes.

using Eq. (33) and the values obtained using Eqs. (36a,b) for $N = 10$ and $N = 100$. Note the overlapping region where both Eqs. (36a,b) are accurate. Clearly the expression of N_k^* above has the correct limits in that $N_k^* = N$ as $\gamma \to 0$ and $N_k^* = 1$ when $\gamma \to \infty$. Note that there also exists a relatively linear transition region where the mode is changing from being extended to being strongly localized. In their linear region, N^* is found to be proportional to the inverse of γ, that is $N^* = 2/\gamma$. Therefor N^* is a direct measure of the decay length scale in the transition region indicating the tip displacements drop off from a peak with the form $e^{-(2/N^*)n}$.

Numerical Results and Discussion

In Ref. 6, it was seen that the localization of a mode as a function of increasing imperfection strength is a relatively smooth process except when curve veering occurs. Results of a 10-rib structure with $k_c = 3\ EI/l^3$ are shown in Figs. 4 and 5. In these figures, the tip displacement of the ribs are plotted for different levels of random imperfections in the rib flexural stiffness. The imperfection strength refers to the limits of $\Delta EI/EI$. Figures 4 and 5 emphasize the fact that mode localization in structures with relatively few substructures can depend strongly on the particular set of random imperfections present, and their geometric relationship to each other. Figure 4 shows the progressive localization of the $n = 0$ mode of the third mode group, where n is the circumferential wave number, and no curve veering occurred. The mode can be seen to localize in a relatively smooth manner. When curve veering occurs, two eigenvalues come very close together but then veer away from each other as the imperfection strength is increased. An important characteristic of curve veering is that the eigenfunctions associated with the eigenvalues before veering are interchanged during veering in a rapid but continuous way.[13] Figure 5 shows the progressive localization of the $n = 0$ mode of the second mode group when the *exact same ribs* used in Fig. 1 are rearranged. For this case the frequency evolution has an example of curve veering as is evidenced by the abrupt change that occurs in the location of the peak of the localized mode. Note the difference in the way the modes localize, although the end result is still a peak on the rib with the lowest flexural stiffness. It is important to emphasize that the only difference between the structures analyzed in Figs. 4 and 5 is the ribs are rearranged.

Figure 6 shows how L^* varies as a function of the imperfection strength for the modes shown in Figs. 4 and 5. Note that L^* is basically the fraction of ribs participating in the mode. Even though the mode undergoes an abrupt change between the imperfection strengths of $\pm 1.5\%$ and $\pm 2.5\%$ in Fig. 5, L^* remains a smooth function. The modes appear to localize in roughly a logarithmic manner as a function of the imperfection strength. It can be seen from Fig. 6 that case 1 begins to localize more quickly than case 2, but after the curve veering case 2 is more localized, although by the time $L^* < 0.3$ both cases are strongly localized.

Modes within the same mode group can have significantly different degrees of localization. In Fig. 7, L^* is shown for the modes in the first three mode groups of an 18-rib structure with $k_c = 3EI/l^3$ and random imperfections of $\pm 2.5\%$. Note that this spring stiffness is 10 times greater than the k_c that was required to match the frequencies presented in Ref. 14 as shown in Ref. 6. Since the structure studied has 18 ribs there will be 18 modes per mode group. In the first mode group, the ribs are primarily in first bending. Similarly, the ribs in the second and third mode groups are primarily in second and third bending, respectively. Figure 7 shows that the first mode group is not localized whereas every mode in the third mode

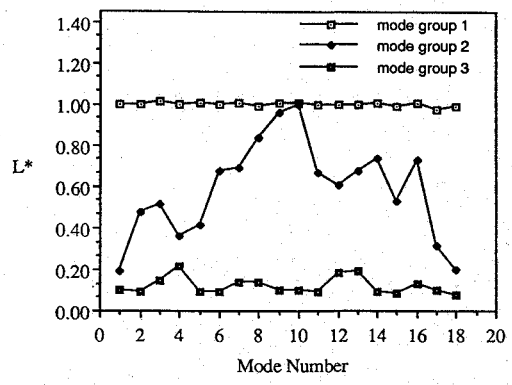

Fig. 7 Variation of the degree of localization within a mode group. All the modes of the third mode group are strongly localized, and the second mode group has both localized and extended modes. All of the modes of the first mode group remain extended, ($N = 18$, $k_c = 3EI/l^3$).

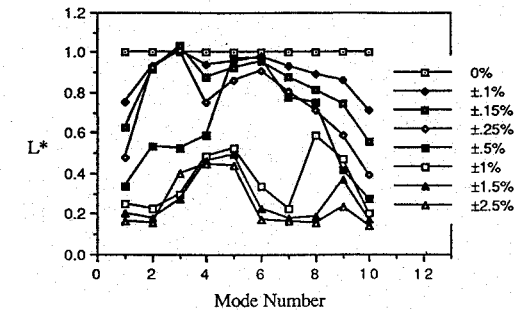

Fig. 8 Variations of L^* for all the modes in the third mode group. Note that L^* decreases monotonically at the ends of the bands, but the center of the band is much more complicated ($N = 10$, $k_c = 3EI/l^3$).

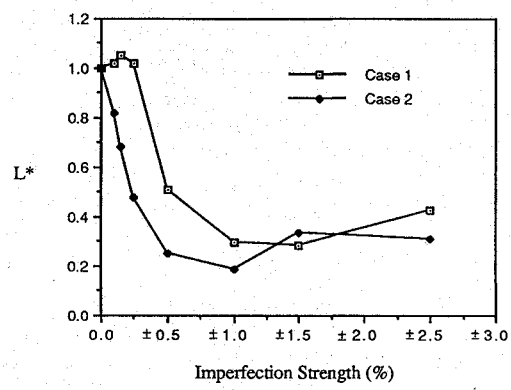

Fig. 9 The strong dependence on the particular set of ribs present in the structure is illustrated for the third mode in the third mode group when $N = 10$ and $k_c = 3EI/l^3$. The only difference between case 1 and case 2 is the ribs have been rearranged.

group has an $L^* < 0.20$. Converting this to the number of ribs participating in the mode for this structure results in less than four of the ribs having any significant amplitude. Therefore, all of the modes in the third mode group are strongly localized. The second mode group is found to lie between these two extremes. For the second mode group, the band edges are strongly localized whereas the center of the band is still extended. This behavior of the band edges becoming localized first was also presented by Pierre[7] in regard to the localization of a linear chain of SDOF oscillators using a transfer matrix approach as well as a modal formulation.

The transition of an entire mode group from being extended to being localized is shown in Fig. 8. In Fig. 8, the change in L^* is shown as a function of the imperfection strength for all

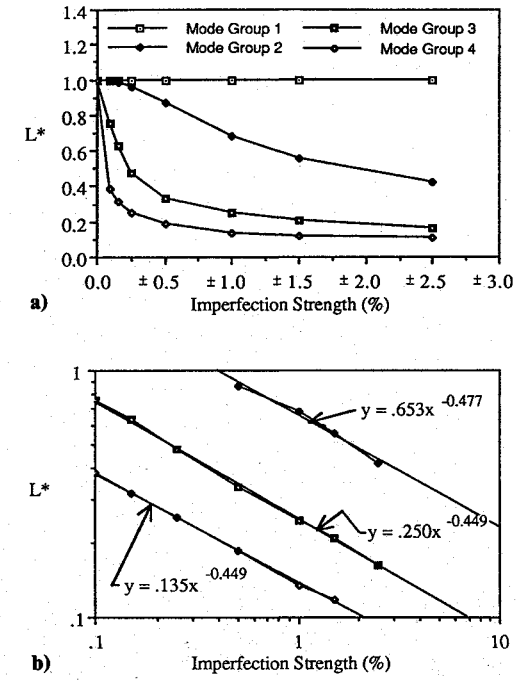

Fig. 10 Illustration of a relationship that exists for the location of the umbrella mode of the first four mode groups ($N = 10$, $k_c = 3EI/l^3$).

of the modes in the third mode group when the number of ribs is equal to 10 and the coupling $k_c = 3EI/l^3$. Note that for the ends of the band, L^* is monotonically decreasing whereas the other modes in the mode group have a much more complex behavior, and depends on the exact ribs used and their relationship to each other. In general, it can be seen that the ends of the band become localized faster (that is at a lower imperfection strength) than the modes in the center of the band.

In Fig. 9, L^* for the third mode in the third mode group is presented for two cases of random imperfections. Once again, the only difference between the two cases is that the ribs are rearranged. Note the modes become localized in very different manners. For example, at an imperfection strength of ±0.25% the mode of case 1 is still extended, whereas the mode for case 2, less than half of the substructures have any significant amplitude. These results reinforce the position that analytical results derived using the limit as the number of substructures goes to infinity must be viewed with caution, when applied to finite structures, and may be extremely inaccurate for a particular structure. As Pierre emphasized in Ref. 12, we are interested in the behavior of individual disordered structures as much as the average of an ensemble of structures. Some values of L^* shown in Fig. 9 are greater than one. One important effect of imperfections is to couple the modes that were orthogonal to each other in the perfect structure.[4] In this particular example, for small values of the imperfection strength, the umbrella mode of the third mode group and the third mode of the third mode group were coupled so as to make the third mode of the disordered structure look more extended than the third mode of the perfect structure (i.e., $L^* > 1$). Remember for the third mode of the perfect structure $N^* = 6.67$ as given by Eq. (35), and $N^* = 10$ for the umbrella mode of the perfect structure. Therefore, when calculating L^* in Eq. (34) a different number is used in the denominator.

A relationship exists for the localization of modes in different mode groups which have the same circumferential wave number as illustrated in Fig. 10 for a 10-rib structure with $k_c = 3EI/l^3$. Figure 10a is a plot of L^* for the umbrella ($n = 0$) mode as a function of the imperfection strength for the first four mode groups. If the transition region between being extended to being strongly localized on one substructure is plotted on a log-log scale, a definite relationship is seen be-

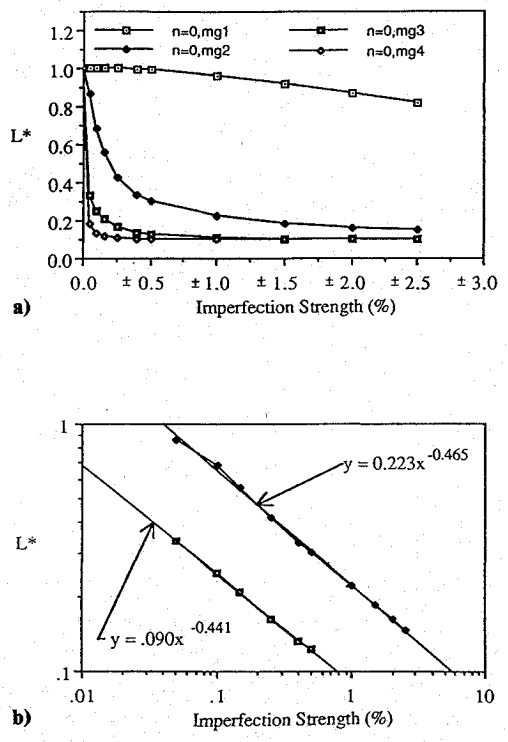

Fig. 11 Same as Fig. 10 except the coupling has been reduced to $k_c = 0.3EI/l^3$. Note that the curves for the second and third mode groups have simply shifted to the left.

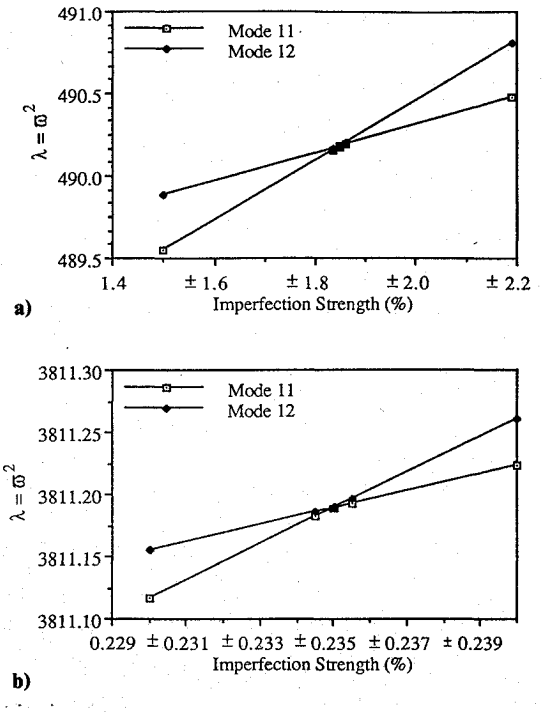

Fig. 12 Part of the frequency evolution of the 11th and 12th modes of the second and third mode groups illustrating a veering between the modes of both mode groups. The imperfection strength at which the veering occurs for the two mode groups are related by Eq. (39) ($N = 18$, $k_c = 298EI/l^3$).

tween the mode groups as shown in Fig. 10b, where L_k^* is seen to follow a power-law relationship of the form:

$$L_k^* = a_j r^{-c_1} \tag{37}$$

where c_1 is a constant depending on which mode in the mode group is being examined, and the coefficient a_j varies from one mode group to another. The umbrella mode for the first mode group is not included in Fig. 10b since it is still extended at an imperfection strength of ± 2.5%. Equation (37) can be rearranged to express the imperfection strength in terms of L_k^*:

$$r = \left(\frac{a_j}{L_k^*}\right)^{1/c_1} = b_j (L_k^*)^{c_2} \tag{38}$$

The ratio b_j/b_{j+1} is approximately equal to $\Delta\lambda_j/\Delta\lambda_{j+1}$. Therefore, for a given L_k^* we know

$$\frac{r_j}{r_{j+1}} = \frac{b_j}{b_{j+1}} \approx \frac{\Delta\lambda_j}{\Delta\lambda_{j+1}} \tag{39}$$

For example, if one knows that the umbrella mode of the second mode group has an $L^* = 0.5$ at an imperfection strength of $r_2 = \pm 1.8\%$, then Eq. (37) could be used to find the imperfection strength for which the higher mode groups have an $L^* = 0.5$. For very flexible cyclic structures that are characterized by widely spaced mode groups, the possibility exists for modeling one mode group as a series of SDOF oscillators and then use the theoretical results available for such structures. The behavior of the higher mode groups can then be inferred using $\Delta\lambda_j$ as a scaling parameter.

Changing the coupling would be expected to have roughly the same effect as changing the imperfection strength, since it is the ratio of the coupling to the imperfection strength that is expected to be the important parameter.[4] Therefore, changing the coupling strength should just shift the curves shown in Fig. 10 to the left, that is the modes will localize at a lower imperfection strength. This indeed turns out to be the case as shown in Fig. 11, which shows L^* as a function of the imperfection strength for the first four mode groups of a 10-rib structure with $k_c = 0.3EI/l^3$. The transition region for the $n = 0$ mode of the second and third mode groups is shown in Fig. 11b. From Fig. 11a, it can be seen at the $n = 0$ mode of the fourth mode group localizes at a very low imperfection strength and is therefore not included in Fig. 11b since only two calculated values fell in the transition region. As can be seen by the curve fits shown in this figure, changing the coupling has essentially only changed the coefficients a_j in Eq. (37) by making them smaller. By making the educated guess that the coupling-to-disorder ratio should be a term in Eq. (37), and using the observation shown in Eq. (39), it was discovered that all of the curves shown in Figs. 10 and 11 can be expressed in a single equation fairly accurately. If we assume the exponent in the power-law relationship is $c_1 = 0.449$, we find for the umbrella mode of the jth mode group

$$L^* = 6.4 \left[\frac{k_c}{r\lambda_{j0}}\right]^{0.449} \tag{40}$$

where λ_{j0} is the normalized squared frequency of the jth cantilever beam bending mode, or in terms of the normalized eigenvalue band:

$$L^* = 1.78 \left[\frac{\Delta\lambda_j}{r}\right]^{0.449} \tag{41}$$

where again $\Delta\lambda_j$ is the normalized eigenvalue band for the jth mode group which will be a function of the coupling strength and the displacement at the coupling location.

It is important to emphasize that these coefficients and exponents were obtained using a single set of random numbers to generate the random variation in EI, and one would not necessarily expect these precise values when a different set of random imperfections is used. In the transition region, no theoretical results are available for localization factors, because all perturbation schemes break down.[12] Therefore, it is not surprising that the functional relationship between L^* and r is clearly different than what is predicted using theoretical

results for weak localization obtained for systems of infinite extent which can be modeled by a product of 2×2 transfer matrices. As shown earlier, in the transition region $N^* = N_0^*$, L^* is proportional to the inverse of the localization factor γ. It has been shown[11] that in the case of *weak* localization, γ is of the form

$$\gamma = \frac{\sigma^2}{8\, k_c^2\, (1 - A^2/4)} \tag{42}$$

where σ^2 is the variance of the random variable and the system is of infinite extent and can be modeled by a 2×2 transfer matrix of the form

$$[T_i] = \begin{bmatrix} A & -1 \\ 1 & 0 \end{bmatrix} \tag{43}$$

The term "A" is a function of the frequency ω and the other parameters of the particular system being modeled. Therefore, in the case of weak localization, $1/\gamma$ is proportional to $1/\sigma^2$ and therefore proportional to $1/r^2$ because of the way the imperfection strength is defined. This is clearly in contrast to this numerical simulation that shows that $1/\gamma$ is approximately proportional to $1/r^{0.45}$ in the transition region for this structure of finite extent. Again, the exponent is only approximate. These results emphasize the importance of recognizing the assumptions involved in a perturbation scheme and only applying the perturbation results in circumstances where the assumptions are valid.

Equation (39) is also valid for comparing the frequency evolution of the various mode groups. For example, in Fig. 12a, a part of the frequency evolution as a function of the imperfection strength is shown of the 11th and 12th modes in the second mode group of an 18-rib structure with $\bar{k}_c = 0.298$ EI/l^3. Note that the frequencies veer away from each other at an imperfection strength of approximately $\pm 1.848\%$. Using the relationship shown in Eq. (39), we calculate that the 11th and 12th modes of the 3rd mode group should veer at an imperfection strength of approximately

$$r_3 \approx \frac{\Delta\lambda_3}{\Delta\lambda_2} r_2 = \pm 0.235\%$$

which indeed turns out to be the case as is shown in Fig. 12b.

Conclusions

The following main conclusions can be drawn for the class of disordered cyclic structures examined in this study:

1) The particular set of random imperfections introduced into a finite cyclic structure can strongly influence the manner in which the modes become localized.

2) Modes within the same mode group can have significantly different degrees of localization with some modes being strongly localized while others remain extended.

3) The spatial extent of a mode as it progressively localizes with increasing imperfection strength appears to obey a power-law-type relationship in the transition region, when the spatial extent of the mode is measured by L^*. The localization length scale provides insight into the transition region, while the anaytical approach fails in this region.

4) The localization length scale L^* describes the spatial extent of a mode and is useful for studying the transition from extended to localized states. In the transition region, L^* is proportional to $1/\gamma$.

5) The normalized eigenvalue band accurately reflects the coupling for a mode group and can be used as a scaling parameter to predict the behavior of other mode groups when the behavior of one mode group is known.

Appendix

The mode shapes used in the Rayleigh-Ritz formulation as shown in Eq. (1) are given by

$$\phi_n = \cosh\beta_n\bar{x} - \cos\beta_n\bar{x} - \alpha_n(\sinh\beta_n\bar{x} - \sin\beta_n\bar{x}) \tag{A1}$$

where

$$\beta_1 = 1.875104, \quad \alpha_1 = 0.7340955 \tag{A2a}$$

$$\beta_2 = 4.694091, \quad \alpha_2 = 1.018466 \tag{A2b}$$

$$\beta_3 = 7.854757, \quad \alpha_3 = 0.9992245 \tag{A2c}$$

$$\beta_4 = 10.99554, \quad \alpha_4 = 1.000034 \tag{A2d}$$

$$\beta_5 = 14.13717, \quad \alpha_5 = 0.9999986 \tag{A2e}$$

The natural frequencies for the first five cantilevered beam modes are found to be

$$\omega_n = \beta_n^2 \sqrt{EI/ml^4} \tag{A3}$$

When Eq. (A3) is nondimensionalized by ω_0, the values of the eigenvalues are

$$\lambda_{1_0} = \bar{\omega}_1^2 = 12.36236 \tag{A4a}$$

$$\lambda_{2_0} = \bar{\omega}_2^2 = 485.51876 \tag{A4b}$$

$$\lambda_{3_0} = \bar{\omega}_3^2 = 3806.54542 \tag{A4c}$$

$$\lambda_{4_0} = \bar{\omega}_4^2 = 14{,}617.26940 \tag{A4d}$$

$$\lambda_{5_0} = \bar{\omega}_5^2 = 39{,}943.84996 \tag{A4e}$$

The normalized eigenvalue band for the five mode groups are shown below

$$\Delta\lambda_1 = 0.3092 \tag{A5a}$$

$$\Delta\lambda_2 = 0.0099 \tag{A5b}$$

$$\Delta\lambda_3 = 0.00126 \tag{A5c}$$

$$\Delta\lambda_4 = 0.000326 \tag{A5d}$$

$$\Delta\lambda_5 = 0.000119 \tag{A5e}$$

References

[1]Hodges, C. H., "Confinement of Vibration by Structural Irregularity," *Journal of Sound and Vibrations,* Vol. 82, No. 3, 1982, pp. 411–424.

[2]Bendiksen, O. O., "Aeroelastic Stabilization by Disorder and Imperfections," XVI International Congress of Theoretical and Applied Mechanics, Paper 583P, Lyngby, Denmark, Aug. 1984.

[3]Pierre, C., "Analysis of Structural Systems with Parametric Uncertainties," Ph.D. Thesis, Dept. of Mechanical and Aerospace Engineering and Materials Science, Duke Univ. Durham, NC, July 1985.

[4]Bendiksen, O. O., "Mode Localization in Large Space Structures," *AIAA Journal,* Vol. 25, Sept. 1987, pp. 1241–1248.

[5]Pierre, C., Tang, D. M., and Dowell, E. H., "Localized Vibrations of Disordered Multispan Beams: Theory and Experiment," *AIAA Journal,* Vol 25, Sept. 1987, pp. 1249–1257.

[6]Cornwell, P. J., and Bendiksen, O. O., "Localization of Vibrations in Large Space Reflectors," *AIAA Journal,* Vol. 27, No. 2, pp. 219–226.

[7]Pierre, C., "Strong Mode Localization in Nearly Periodic Disordered Structures," *AIAA Journal,* Vol. 27, No. 2, pp. 227–241.

[8]Painter, R. D., and Hartmann, W. M., "Localization of the Vibrational States of Binary Disordered Linear Chains," *Physical Review B,* Vol. 13, No. 2, 1976, pp. 479–491.

[9]Papatriantafillou, C., Economou, E. N., and Eggarter, T. P., "Eigenfunction in One-Dimensional Disordered Systems, I and II," *Physical Review B,* Vol. 13, No. 2, 1976, pp. 910–928.

[10]Moore, E. J., "Numerical Studies of the One-Dimensional Random Anderson Model," *Journal of Physics C: Solid State Physics,* Vol. 6, 1973, pp. 1551–1558.

[11]Kissel, G. J., "Localization in Disordered Periodic Structures," *Proceedings of the 27th AIAA/ASME/ASCE/AHS Structures, Structural Dynamics and Materials Conference,* AIAA, New York, 1987, pp. 1046–1055.

[12]Pierre, C., "Weak and Strong Vibration Localization in Disordered Structures: A Statistical Investigation," *Proceedings of the 28th AIAA/ASME/ASCE/AHS Structures, Structural Dynamics and Materials Conference,* AIAA, Washington, DC, 1988.

[13]Perkins, N. C., and Mote, C. D., "Comments on Curve Veering in Eigenvalue Problems," *Journal of Sound and Vibrations*, Vol. 106, No. 3, 1986, pp. 451–463.

[14]El-Raheb, M., and Wagner, P., "Static and Dynamic Characteristics of Large Deployable Space Reflectors," *Proceedings of the AIAA/ASME/ASCE/AHS 22nd Structures, Structural Dynamics and Materials Conference,* AIAA, New York, 1981, pp. 77–84..